

Discovery of Phosphodiesterase 10A (PDE10A) PET Tracer AMG 580 to Support Clinical Studies

Essa Hu,^{*,†} Ning Chen,[†] Roxanne K. Kunz,[†] Dah-Ren Hwang,^Δ Klaus Michelsen,[⊥] Carl Davis,[‡] Ji Ma,[±] Jianxia Shi,[±] Dianna Lester-Zeiner,^{||} Randall Hungate,[†] James Treanor,[§] Hang Chen,^{||} and Jennifer R. Allen[†]

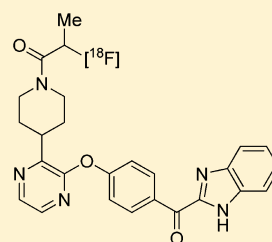
[†]Department of Medicinal Chemistry, [‡]Department of Pharmacokinetics and Drug Metabolism, [§]Department of Neuroscience, and ^ΔDepartment of Early Development, Amgen Inc., One Amgen Center Drive, Thousand Oaks, California 93012-1799, United States

^{||}Department of Neuroscience and [±]Department of Pharmacokinetics and Drug Metabolism, Amgen Inc., 1120 Veterans Boulevard, South San Francisco, California 94080, United States

[⊥]Department of Molecular Structure and Characterization, Amgen Inc., 360 Binney Street, Cambridge, Massachusetts 02142, United States

S Supporting Information

ABSTRACT: We report the discovery of PDE10A PET tracer AMG 580 developed to support proof of concept studies with PDE10A inhibitors in the clinic. To find a tracer with higher binding potential (BP_{ND}) in NHP than our previously reported tracer **1**, we implemented a surface plasmon resonance assay to measure the binding off-rate to identify candidates with slower washout rate in vivo. Five candidates (**2–6**) from two structurally distinct scaffolds were identified that possessed both the in vitro characteristics that would favor central penetration and the structural features necessary for PET isotope radiolabeling. Two cinnolines (**2, 3**) and one ketobenzimidazole (**5**) exhibited PDE10A target specificity and brain uptake comparable to or better than **1** in the in vivo LC–MS/MS kinetics distribution study in SD rats. In NHP PET imaging study, [¹⁸F]-**5** produced a significantly improved BP_{ND} of 3.1 and was nominated as PDE10A PET tracer clinical candidate for further studies.



compound [¹⁸F]-**5**
PDE10A IC_{50} = 0.1 nM
LC-MS/MS, $AUC_{Str/Tha}$ = 23
LC-MS/MS, %ID/g = 1.2%
NHP PET striatum BP_{ND} = 3.1

KEYWORDS: Phosphodiesterase, tracer, receptor occupancy, positron emission tomography, radiotracer, brain penetration

Positron emission tomography (PET) imaging using a radiolabeled tracer is a direct and noninvasive technology platform that has found broad utility in the clinic. Some well-known examples include: 2-[¹⁸F]-fluoro-2-deoxy-D-glucose (FDG) used to measure tumor metabolism to monitor cancer progression, [¹¹C]-2-(4-(methylamino)phenyl)-6-hydroxybenzothiazol (PIB) and [¹⁸F]-florbetaben designed to assess β -amyloid plaque accumulation in the brain to diagnose Alzheimer's disease, and [¹¹C]-raclopride and [¹⁸F]-fallypride designed to quantify target occupancy (TO) at dopamine receptors to enable correlation of TO with clinical end points or adverse events. For novel therapeutic agents targeting the central nervous system (CNS), PET imaging provides an assessment of CNS target engagement more directly than other readouts such as biomarker levels in the plasma or the cerebral spinal fluid (CSF). Nevertheless, it is still uncommon for research groups to develop both a novel, therapeutic agent and a novel, target specific PET tracer in parallel due to cost, time, and resource limitations.¹

When we initiated a drug discovery effort to develop a phosphodiesterase 10A (PDE10A) inhibitor, it quickly became apparent that the profile of this CNS target was particularly suitable for tracer development. PDE10A belongs to a family of 11 isoforms found to be highly compartmentalized in the body.

PDE10A, in particular, is reported to be most highly expressed in the striatum medium spiny neuron (MSN), a region of the brain that has been associated with the pathophysiology of schizophrenia. Reports of the high density and localization of PDE10A in the brain suggested likelihood of a strong and specific PET signal essential for imaging and TO calculations. Functionally, phosphodiesterases hydrolyze the 3'-5' phosphodiester bonds on secondary messengers cyclic adenosine monophosphate (cAMP) and cyclic guanine monophosphate (cGMP) to convert them into adenosine monophosphate (AMP) and guanine monophosphate (GMP). Microdialysis and microwave methods have been reported for measuring the changes of cAMP/cGMP levels in vivo as a means to assess the efficacy of drug candidates in preclinical species. However, these methodologies would not be translatable to the clinic. Having a selective PDE10A tracer would not only demonstrate target engagement by CNS TO but also enable translation of preclinical to clinical findings. The value of having PDE10A

Received: May 3, 2016

Accepted: May 19, 2016

PET tracers in the clinic has been echoed in the research community as reflected by recent tracer publications.¹

Once we decided to develop a PDE10A radiotracer, we explored various approaches to expedite the tracer discovery process in hopes of reducing resource burden. Recently, we reported the rapid identification of PDE10A tracer 5-(6,7-dimethoxycinnolin-4-yl)-*N*-isopropyl-3-methylpyridin-2-amine (AMG 7980, **1**) using a combination of preselected in vitro characteristics to favor central uptake and liquid chromatography-tandem mass spectrometry (LC-MS/MS) technology to quantify compound exposures down to microgram levels in brain tissues (Figure 1).² The utility of tracer **1** was

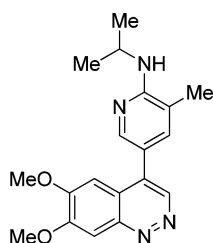


Figure 1. PDE10A tracer **1**.

demonstrated in an in vivo rodent TO study with a structurally distinct PDE10A inhibitor. With a capacity of four compounds every 2 weeks, this LC-MS/MS TO measurement platform using tracer **1** provided the critical path study for in vivo evaluation of our own PDE10A candidates in-house.^{3–5}

Unfortunately, our hope to advance **1** as a PDE10A PET tracer could not be realized as [¹¹C]-**1** exhibited suboptimal binding potential with respect to the nondisplaceable tracer concentration (BP_{ND}) of 0.62 by simplified reference tissue model (SRTM) and 0.9 by one tissue compartment model (1TC) in a nonhuman primate (NHP) PET imaging study.⁶ Since a radiotracer's BP_{ND} value is proportional to the level of precision of its TO measurements, we decided **1** would not be sufficient to support our clinical studies. Analysis of the PET imaging data revealed excellent brain uptake of [¹¹C]-**1** but also a fast wash out rate. We hypothesized that increasing the tracer target retention time would address the issue. Thus, a renewed effort was initiated to find a PET tracer candidate with improved BP_{ND}. This report describes the initial hypothesis, strategy, screening, selection, and design that led to the identification of PET tracer clinical candidate AMG 580. Additional profiling of the candidate both in vitro and in vivo, across various species and in PET imaging studies, have been reported in separate communications.^{7,8}

This time, we expanded the scope of structural diversity to include multiple scaffolds investigated by our in-house PDE10A inhibitor discovery efforts (see Supporting Information for flow scheme).^{3–5,9–11} Historical compounds were filtered based on a specific set of in vitro parameters that favor brain penetration: (1) PDE10A binding affinity comparable to or better than **1** (PDE10A IC₅₀ = 1.9 nM), (2) PDE selectivity greater than 100-fold against the rest of the PDE isoforms (1–9, 11), (3) permeable, and (4) low P-gp efflux ratio. Candidates must also possessed the molecular structures amenable to radiolabeling with PET isotopes [¹¹C] or [¹⁸F].^{12–14} New analogues were designed based on our reported cocrystal structures, which revealed a potential benefit from exploiting the solvent exposed regions of the PDE10A binding domain. We hypothesized that decreasing the binding off rate of the tracer candidates could

reduce the wash out rate observed in the NHP PET study. Thus, a surface plasmon resonance (SPR) binding assay was incorporated into the flow scheme to assess the binding kinetics. Based on the formula $\{T_{1/2} = \ln(2)/k_d\}$, compounds with binding half-life, $T_{1/2}$, at least 5-fold longer than **1** ($T_{1/2} = 0.04$ min) were advanced into the in vivo LC-MS/MS kinetics study. Binding specificity was quantified as a ratio of a compound's area under the curve (AUC) in the target region (striatum; Str) over the control region (thalamus; Tha). Brain uptake was calculated as the percentage of injected dose measured in the target region per gram of tissue (%ID/g). Five structurally distinct and novel analogues emerged as a result of the LC-MS/MS study (Figure 2). In this report, we describe

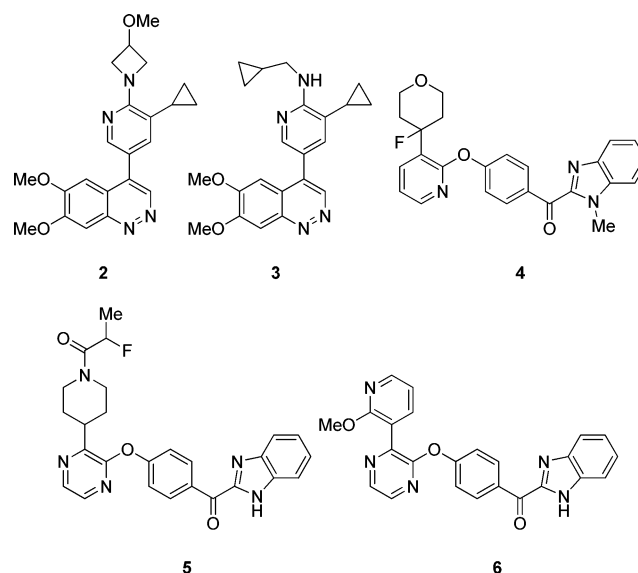


Figure 2. Structures of five distinct PDE10A inhibitors **2–6** as tracer candidates.

these five lead candidates, their in vitro and in vivo profiles, and the identification of one suitable PDE10A PET tracer as a clinical candidate. Synthetic routes used to make tracer candidates **2–6** are described in the Supporting Information section.

In the in vivo LC-MS/MS kinetics study, all five candidates exhibited good levels of specificity for PDE10A enriched striatum over thalamus ($AUC_{Str/Tha} > 5$) and good brain uptake (%ID/g > 0.5) (Table 1 and Figure 3).¹⁵ In the PDE10A biochemical assay, the new analogues exhibited IC₅₀ values ranging from 1.7 nM (activities comparable to **1**) to 0.1 nM (nearly 20-fold more potent than **1**). The magnitude of increase in the biochemical activity did not always correlate with improvement in the binding $T_{1/2}$. Cinnoline **2** exhibited PDE10A activity similar to tracer **1**, and yet, its binding off-rate was 6-fold slower compared to **1**. Although cinnoline **3** was 7-fold more potent than keto-benzimidazole **4** in the PDE10A assay, its binding $T_{1/2}$ was only 21-fold longer compared to the 32-fold binding $T_{1/2}$ improvement observed with **4**. The most dramatic difference was found with keto-benzimidazole **6**, with a PDE10A IC₅₀ of 0.3 nM and an 85-fold increase in binding $T_{1/2}$. Not surprisingly, improvements in binding off-rate were not reflected in the striatum to thalamus ratio as these measurements were taken at a single time point of 10 min after compound dosing. Nevertheless, the striatum to thalamus ratio was one preliminary indicator of the signal-to-noise ratio in the

Table 1. Profile of Five Lead Candidates 2–6 That Exhibited Improved Binding $T_{1/2}$, Good Specificity in PDE10A Enriched Region in CNS, and Good Brain Uptake

compd	PDE10A IC ₅₀ (nM)	binding $T_{1/2}$ (fold) ^a	LC–MS/MS TO ^b	
			[AUC _{Str/Tha}] ^c	[%ID/g] ^d
1	1.9	1×	9.4	1.2
2	1.7	6×	12.6	0.8
3	0.1	21×	8.7	0.8
4	0.7	32×	5.6	0.3
5	0.1	16×/61× ^e	23	1.2
6	0.3	85×	5.7	1.0

^aFold over 1. Binding $T_{1/2}$ values were calculated based on measured K_d using the formula: $\{T_{1/2} = \text{Ln}(2)/k_d\}$. ^bLC–MS/MS study was conducted in Sprague–Dawley (SD) rats at $n = 10$ per group. The compounds were dosed i.v. and formulated in 100% DMSO. ^cRatio of AUC of compound in striatum (Str) over AUC of compound in thalamus (Tha) at $t = 10$ min after dosing. ^dPercentage of injected dose (ID) of compound in the striatum per gram of tissue sampled. ^eSee Supporting Information section for additional experimental data on 5.

in vivo PET imaging study. Thus, with tracer 1 as the benchmark, we advanced only compounds 2, 3, and 5,¹⁶ which produced striatum to thalamus ratio comparable or superior to 1.

Prior to in vivo NHP PET imaging study, all three lead candidates were further profiled in rats to make sure the tracer signals were saturable and that the tracer candidates could be blocked by a PDE10A inhibitor. The LC–MS/MS methods utilized were previously described in our report on tracer 1.² As an example, we reported that candidate 5 produced a saturable, specific, in vivo binding kinetics profile in the LC–MS/MS study.⁷ To demonstrate that the tracer can be blocked and thus can be used to measure TO in vivo, we performed an in vivo

LC–MS/MS TO study in SD rats using our recently reported PDE10A clinical candidate, AMG 579,¹⁷ as the blocker. Blocker was administered orally at doses 0.1, 0.3, 1, 3, 10, and 30 mg/kg, 1.5 h before administration of tracer 5 (5 $\mu\text{g}/\text{kg}$ i.v.). Tissues from the striatum and the thalamus, as well as blood samples, were collected after 30 min. Both tracer and blocker levels in the brain tissues were determined by LC–MS/MS. As shown in Figure 4, tracer 5 was able to measure TO with our

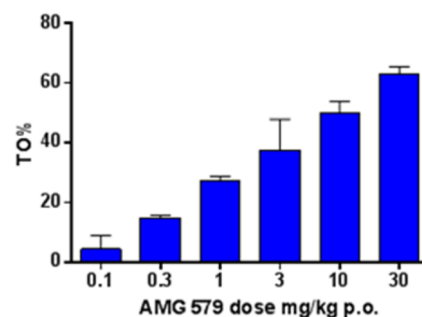


Figure 4. Tracer blocking study using 5 as tracer and PDE10A inhibitor AMG 579 as blocker. Blocker was dosed orally at doses 0.1, 0.3, 1, 3, 10, and 30 mg/kg. Tracer 5 was dosed i.v. at 5 $\mu\text{g}/\text{kg}$ 1.5 h post blocker dosing. Tissues were collected and analyzed 30 min post-tracer dosing. $N = 3$ –4 animals per group.

blocker in a dose-dependent manner, reaching 63% PDE10A occupancy at 30 mg/kg dose. This study confirmed the utility of tracer candidate 5 for in vivo measurement of PDE10A inhibitor TO.⁷

Both cinnoline candidates 2 and 3 were eliminated as a result of the PET imaging study. [¹¹C]-2 exhibited fast washout presumably because the 6-fold improvement in binding $T_{1/2}$ over 1 was not sufficient to have a significant impact on its in vivo off rate. Meanwhile, [¹¹C]-3 formed a significant amount

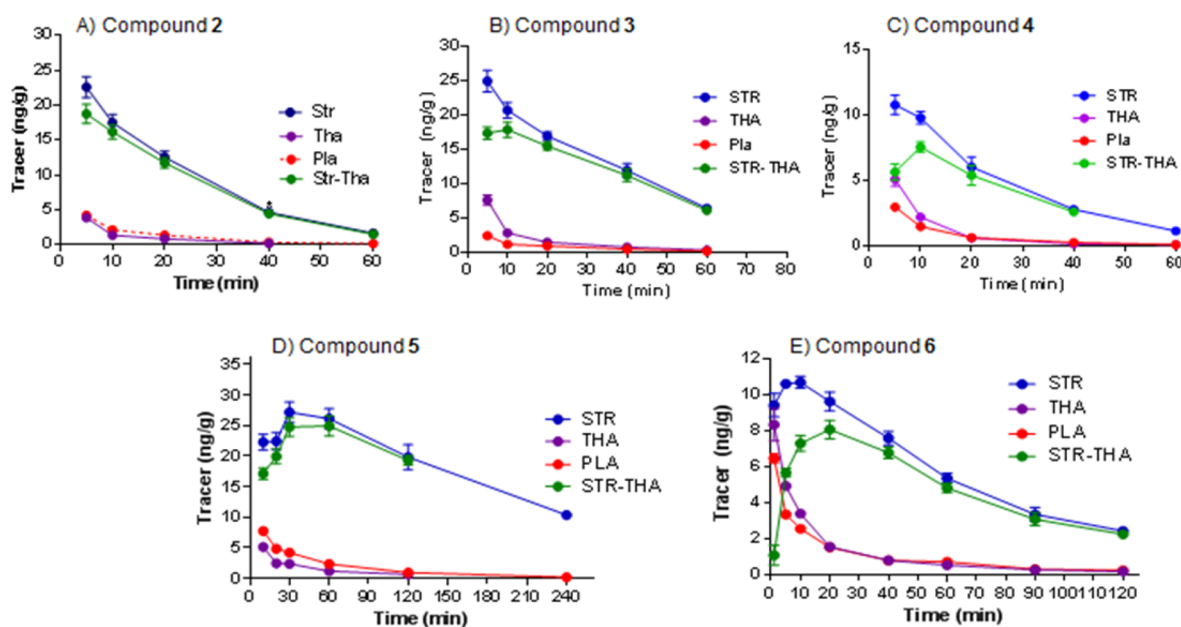


Figure 3. In vivo kinetics distribution of tracer candidates 2–6 in SD rats. Compounds 2–5 were dosed i.v. at 10 $\mu\text{g}/\text{kg}$, while 6 was dosed at 5 $\mu\text{g}/\text{kg}$. The concentration of tracer candidates in the striatum (STR, blue dot), thalamus (THA, purple dot), and plasma (PLA, red dot) were measured by LC–MS/MS. Specific uptake was calculated by subtraction of compound level in the thalamus from compound level in the striatum (STR-THA, green dot). Error bars represent standard error of mean, and $n = 3$ –4 animals per group. In vivo kinetics distribution graphs for tracer candidates (A) 2, (B) 3, (C) 4, (D) 5, and (E) 6.

of brain-penetrant radioactive metabolites in NHP suggesting the molecule was metabolized differently in NHP compared to cinnoline **1**, which was absent of brain penetrant radioactive metabolites. Gratifyingly, [¹⁸F]-**5** produced promising results. In the NHP PET imaging study, [¹⁸F]-**5** exhibited BP_{ND} of 3.1 in the PDE10A rich striatum region by SRTM, which constitutes a significant improvement compared to BP_{ND} of 0.6 for [¹¹C]-**1**. High levels of specific tracer uptake were observed in the PDE10A enriched striatum. Additional details of the NHP PET imaging study along with tissue distribution of [¹⁸F]-**5** have been reported in separate communications.⁸

While developing radiochemistry conditions to make [¹⁸F]-**5** from precursor **10**,¹⁸ we discovered our reaction conditions caused racemization of the stereocenter. This finding made advancement of [¹⁸F]-**5** as a single enantiomer technically challenging. Limited resources precluded us from finding a new radiolabeling condition. Addition of a chiral HPLC separation step after radiosynthesis would lengthen the PET tracer production time and significantly reduce the overall radiochemical yield. Since both enantiomers of **5** exhibited the desired kinetics profiles when profiled as cold compounds by LC–MS/MS (see [Supporting Information](#)), we assessed the option of advancing [¹⁸F]-**5** as a racemate by putting the compound in a battery of profiling studies and in vivo target occupancy studies in both rats and NHP.^{7,8} The data showed **5** was well behaved in vivo and could be modeled well. Thus, we advanced [¹⁸F]-**5** as our clinical PET tracer candidate.

Having a PET imaging tracer to support clinical proof of concept studies is a valuable asset to any CNS drug development program. This noninvasive technology provides a direct means to demonstrate target engagement in the brain in clinical trials and facilitates translation of preclinical findings. Our first PDE10A tracer (**1**) exhibited fast washout in vivo resulting in BP_{ND} < 1 in the NHP PET imaging study. Since BP_{ND} is a critical parameter that impacts both the confidence and the resolution of the PET TO measurement we set out to identify a better PDE10A PET imaging tracer. Historical analogues from several structurally distinct scaffolds in-house were filtered, and novel compounds were designed to find candidates that would meet our preselected in vitro criteria. To identify candidates with slower off rates than **1**, binding T_{1/2} was assessed by an SPR spectroscopy binding assay. Three of the five compounds profiled in the in vivo LC–MS/MS kinetics study achieved in vivo target specificity (AUC_{Str/Tha}) and brain uptake (%ID/g) comparable or better than **1**. All three candidates (**2**, **3**, and **5**) exhibited saturable and specific binding in SD rats in vivo and enabled the measurement of PDE10A inhibitor TO in vivo. When advanced into the in vivo NHP PET imaging study, [¹⁸F]-**5** emerged as the superior tracer candidate exhibiting the desired slower washout rate, minimal radioactive metabolite uptake in the brain, and high BP_{ND} of 3.1 in the striatum. With our goal of finding a PDE10A PET tracer with better BP_{ND} than **1** achieved, [¹⁸F]-**5** was advanced into clinical studies as AMG 580.

■ ASSOCIATED CONTENT

● Supporting Information

The Supporting Information is available free of charge on the [ACS Publications website](#) at DOI: [10.1021/acsmedchemlett.6b00185](https://doi.org/10.1021/acsmedchemlett.6b00185).

Additional experimental data on compound **5**, flow scheme, chemical syntheses of compounds **2–6** and

[¹⁸F]-**5**, experimental methods, and additional references ([PDF](#))

■ AUTHOR INFORMATION

Corresponding Author

*Phone: 805-313-5300. E-mail: ehu@amgen.com.

Notes

The authors declare no competing financial interest.

■ ABBREVIATIONS

ITC, one tissue compartment model; BP_{ND}, binding potential nondisplaceable; CNS, central nervous system; DAST, diethylaminosulfur trifluoride; DCM, dichloromethane; DME, dimethoxyethane; EtOAc, ethyl acetate; LC–MS/MS, liquid chromatography–tandem mass spectrometry; NHP, nonhuman primates; PDE, phosphodiesterase; PET, positron emission tomography; SEM, standard error of the mean; SPR, surface plasmon resonance; SRTM, simplified reference tissue model; THF, tetrahydrofuran; TO, target occupancy

■ REFERENCES

- (1) See [Supporting Information](#) section for additional references on PDE10A and PET imaging technology.
- (2) Hu, E.; Ma, J.; Biorn, C.; Lester-Zeiner, D.; Cho, R.; Rumpf, S.; Kunz, R. K.; Nixey, T.; Michelsen, K.; Miller, S.; Shi, J.; Wong, J.; Hill Della Puppa, G.; Able, J.; Talreja, S.; Hwang, D.-R.; Hitchcock, S. A.; Porter, A.; Immke, D.; Allen, J. R.; Treanor, J.; Chen, H. Rapid identification of a novel small molecule phosphodiesterase 10A (PDE10A) tracer. *J. Med. Chem.* **2012**, *55*, 4776–4787.
- (3) Rzaa, R. M.; Frohn, M. J.; Andrews, K. L.; Chmait, S.; Chen, N.; Eastwood, H.; Horne, D. B.; Hu, E.; Jones, A. D.; Kaller, M. R.; Kunz, R. K.; Miller, S.; Reichelt, A.; Nguyen, T.; Pickrell, A.; Porter, A.; Monenschein, H.; Davis, C.; Zhao, X.; Treanor, J. J. S.; Allen, J. R. Synthesis and preliminary biological evaluation of potent and selective 2-(3-alkoxy-1-azetidiny)quinolines as novel PDE10A inhibitors. *Bioorg. Med. Chem.* **2014**, *22*, 6570–6585.
- (4) Hu, E.; Kunz, R. K.; Chen, N.; Rumpf, S.; Siegmund, A.; Andrews, K.; Chmait, S.; Zhao, S.; Davis, C.; Chen, H.; Lester-Zeiner, D.; Ma, J.; Biorn, C.; Shi, J.; Porter, A.; Treanor, J.; Allen, J. R. Design, optimization, and biological evaluation of novel keto-benzimidazoles as potent and selective inhibitors of phosphodiesterase 10A (PDE10A). *J. Med. Chem.* **2013**, *56*, 8781–8792.
- (5) Hu, E.; Andrews, K.; Chmait, S.; Zhao, X.; Davis, C.; Miller, S.; Hill Della Puppa, G.; Dovlatyan, M.; Chen, H.; Lester-Zeiner, D.; Able, J.; Biorn, C.; Ma, J.; Shi, J.; Treanor, J.; Allen, J. R. Discovery of novel imidazo[4,5-b]pyridines as potent and selective inhibitors of phosphodiesterase 10A (PDE10A). *ACS Med. Chem. Lett.* **2014**, *5* (6), 700–705.
- (6) Hwang, D.-R.; Hu, E.; Rumpf, S.; Easwaramoorthy, B.; Castrillon, J.; Davis, C.; Allen, J. R.; Chen, H.; Treanor, J.; Abi-Dargham, A.; Slifstein, M. Initial characterization of a PDE10A selective positron emission tomography tracer [¹¹C]AMG 7980 in non-human primates. *Nucl. Med. Biol.* **2014**, *41*, 343–349.
- (7) Chen, H.; Lester-Zeiner, D.; Shi, J.; Miller, S.; Glaus, C.; Hu, E.; Chen, N.; Able, J.; Biorn, C.; Wong, J.; Ma, J.; Michelsen, K.; Hill Della Puppa, G.; Kazules, T.; Dou, H. H.; Talreja, S.; Zhao, X.; Chen, A.; Rumpf, S.; Kunz, R. K.; Ye, H.; Thiel, O. R.; Williamson, T.; Davis, C.; Porter, A.; Immke, D.; Allen, J. R.; Treanor, J. AMG 580: a novel small molecule phosphodiesterase 10A (PDE10A) positron emission tomography tracer. *J. Pharmacol. Exp. Ther.* **2015**, *352*, 327–337.
- (8) Hwang, D. R.; Hu, E.; Allen, J. R.; Davis, C.; Treanor, J.; Miller, S.; Chen, H.; Shi, B.; Narayanan, T. K.; Barret, O.; Alagille, D.; Yu, Z.; Slifstein, M. Radiosynthesis and initial characterization of a PDE10A specific PET tracer [¹⁸F]AMG 580 in non-human primates. *Nucl. Med. Biol.* **2015**, *42*, 654–663.

(9) Hu, E.; Kunz, R. K.; Rumfelt, S.; Chen, N.; Bürl, R.; Li, C.; Andrews, K. L.; Zhang, J.; Chmait, S.; Kogan, J.; Lindstrom, M.; Hitchcock, S. A.; Treanor, J. Discovery of potent, selective, and metabolically stable 4-(pyridin-3-yl)cinnolines as novel phosphodiesterase 10A (PDE10A) inhibitors. *Bioorg. Med. Chem. Lett.* **2012**, *22*, 2262–2265.

(10) Hu, E.; Kunz, R. K.; Rumfelt, S.; Andrews, K. L.; Li, C.; Hitchcock, S. A.; Lindstrom, M.; Treanor, J. Use of structure based design to increase selectivity of pyridyl-cinnoline phosphodiesterase 10A (PDE10A) inhibitors against phosphodiesterase 3 (PDE3). *Bioorg. Med. Chem. Lett.* **2012**, *22*, 6938–6942.

(11) Rzas, R. M.; Hu, E.; Rumfelt, S.; Chen, N.; Andrews, A. L.; Chmait, S.; Falsey, J. R.; Zhong, W.; Jones, A. D.; Porter, A.; Louie, S. W.; Zhao, X.; Treanor, J. J. S.; Allen, J. R. Discovery of selective biaryl ethers as PDE10A inhibitors: improvement in potency and mitigation of Pgp-mediated efflux. *Bioorg. Med. Chem. Lett.* **2012**, *22*, 7371–7375.

(12) Miller, P. W.; Long, N. J.; Vilar, R.; Gee, A. D. Synthesis of ^{11}C , ^{18}F , ^{15}O , and ^{13}N radiolabels for positron emission tomography. *Angew. Chem., Int. Ed.* **2008**, *47*, 8998–9033.

(13) Wong, D. F.; Pomper, M. G. Predicting the success of a radiopharmaceutical for in vivo imaging of central nervous system neuroreceptor systems. *Mol. Imaging Bio.* **2003**, *5*, 350–362.

(14) Pike, V. PET radiotracers: crossing the blood-brain barrier and surviving metabolism. *Trends Pharmacol. Sci.* **2009**, *30*, 431–440.

(15) Experimental methods for the LC–MS/MS kinetics study and the SPR assay were previously described in ref 2.

(16) See [Supporting Information](#) for additional experimental data on the enantiomers of **5** isolated from chiral HPLC purification and reasons for advancement of **5** to further in vivo studies.

(17) Hu, E.; Chen, N.; Bourbeau, M. P.; Harrington, P. E.; Biswas, K.; Kunz, R. K.; Andrews, K.; Chmait, S.; Zhao, X.; Davis, C.; Ma, J.; Shi, J.; Lester-Zeiner, D.; Danao, J.; Able, J.; Cueva, M.; Talreja, S.; Kornecook, T.; Chen, H.; Porter, A.; Hungate, R.; Treanor, J.; Allen, J. R. Discovery of clinical candidate 1-(4-(3-(4-(1H-benzo[d]imidazole-2-carbonyl)phenoxy)pyrazin-2-yl)piperidin-1-yl)ethanone (AMG 579), a potent, selective, and efficacious inhibitor of phosphodiesterase 10A (PDE10A). *J. Med. Chem.* **2014**, *57*, 6632–6641.

(18) Cai, L.; Lu, S.; Pike, V. Chemistry with [^{18}F]fluoride ion. *Eur. J. Org. Chem.* **2008**, *2008*, 2853–2873.